Controller Design for Natural and Robotic Systems with Transmission Delays

Abhay Kataria, Hitay Özbay,* and Hooshang Hemami
Department of Electrical Engineering
Ohio State University
Columbus, Ohio

Received 31 October 2000; revised 15 September 2001; accepted 1 February 2002

Robust stability and two-dimensional trajectory following problems are considered for n-link robotic systems with transmission delays. Such problems appear in telerobotics, where the controller is physically far from the robot, and in neural control of musculoskeletal (biological) systems, where muscle actuation and neural sensing are subject to time delays. A typical second-order nonlinear dynamical model is taken with input and output time delays. In a prior work by the authors, a control strategy was developed for stable movement of the planar linkage system, using the standard Q-parameterization and solving an $\mathcal{H}^\infty$ control problem to determine the free parameter. In this article, a new control scheme is proposed to eliminate the steady-state errors seen in the tracking performance of the controller derived in the earlier work. Simulation examples are shown to demonstrate the effectiveness of the proposed control methodology.

1. INTRODUCTION

Time delays are prevalent in the feedback and feedforward paths of many natural and manmade systems.[5,7,47] The origin of the delays may be in transmission of information back and forth, carrying out of computations or procedures, or reallocation of finite resources.[29] Neural transmission delays were identified in the afferent and efferent paths of the central nervous system (CNS) in humans and animals in the late 1970s.[39] Delays are also inherent in teleoperational and industrial material transporting systems. More recently, effects of delays have become more crucial in telerobotic and real-time and on-line applications of collaborative multisite design, display and control.[48] Many communication and computer networks must deal in an effective way with such delays.[37]

*To whom all correspondence should be addressed; e-mail: ozbay@ee.eng.ohio-state.edu.

Whether these phenomenological delays are pure delays or can be approximated by pure delays (with associative filtering and/or in cascade with other processing), their destabilizing effects on systems and the consequent deterioration of performance cannot be ignored.[26] Effective techniques and design strategies are needed to deal with them.

Early studies of this subject appear in refs. 10 and 42, where predictors are proposed to counteract the delays, achieve stability, and improve system performance. For a comprehensive review, see ref. 41.

Theoretical studies of systems with delays (under certain simplifying assumptions) are carried out in ref. 43. The combination of differential and difference equations represents another theoretical avenue, explored in ref. 13.

A third approach to the study of such systems has been in the context of biological systems—looking at how such systems have dealt with delay issues, and at pathological performance where uncontrollable oscillations and tremor result. One conjectured hypothesis with respect to natural systems is that internal models of the system and the environment exist in the controller. The question of the existence and functioning of internal models in the CNS has been raised by many researchers in the last twenty years.[4,34,45] The question hinges on first identifying such models of the self and the environment, and then verifying and confirming the existence of the required components of such models.

The simplest model of continuous systems involves five kinds of components: algebraic function generators, amplifiers and/or attenuators, summing devices, and (most importantly) a memory element—usually an idealized integrator with respect to time.[6,20,35] Discrete-time systems have an idealized time delay as their memory element.[31] Additionally, any internal or external biological model must account for neural transmission delays of variable duration in the feedforward and feedback (efferent and afferent) paths of the CNS-musculoskeletal system. These delays, in the model, allow for a realistic representation of signal transmission and for compensation for delays.[15] The compensation, alternatively, may involve predictors.[3,38] Duplication of the delays or compensation by prediction enables precise movement and functioning of the system, and stability.[8]

Internal models appear to have been proposed in the context of teleoperations with short delays.[1,27,28] For example, ref. 28 proposes telemonitoring of force feedback and the modification of the dynamics of the system, presumably to correspond to a "locally designed" internal model. The effects of force feedback and force reflection are further discussed in ref. 9. Modeling the environment is discussed more recently in ref. 40, and earlier in refs. 17–19.

To summarize—broadly speaking, three different approaches appear to have been taken to the study of systems with delay: analytical methods, experimental methods, and the study of natural systems. This article combines the first and third approaches by considering a three-link model of a biped, and studying human-like maneuvers by analysis and simulation. For simplicity, the maneuvers do not involve interactions with the environment. Consequently, only the dynamics of the system are considered in the internal models, and the environment and the forces of contact with the environment are neither represented nor included in the system or the internal models.

More specifically, robust stability and tracking performance problems are studied for two-dimensional motion of a three-link robotic system, whose mathematical model consists of a second-order nonlinear ordinary differential equation with sensor and actuator time delays. The emphasis of the article is to develop a linear controller, and to gain analytical and computational insight.[22] It is not our objective to design the neural systems involved or modeled in the CNS,[24,25] nor to optimize the performance of the three-link robotic system by feedforward methods and/or linearization at several points along the trajectory.[23] Nor do we claim that the mathematical and analytical tools utilized in this article are used by the CNS in solving its many intricate control and communication problems. What evolution has done in this regard, we do not understand at this time. Unravelling the mysteries of the CNS and even those of many simpler natural systems is indeed a formidable and challenging task for many generations of scientists and engineers to come.

Examples of current telerobotic systems are cited to motivate and encourage the design of more versatile and capable control systems. Most current telerobotic systems have adequate control because their tasks are slow and simple, and their environments are hazard free. For faster performance and hazardous environments, current position control techniques and slow, sequential algorithms of control may not apply or be adequate. An environment that is hazardous to the stability and performance of the telerobot may demand more complex control strategies. This article is a first step in that direction.

The mathematical model considered here is a stable nonlinear input-output operator. Hence, the usual Q-parameterization method[2] can be employed

to characterize the set of all stabilizing controllers. In ref. 15, this approach was used and an $\mathcal{H}^\infty$ control problem was solved to determine the free controller parameter. Stability robustness against delay uncertainty (and other neglected dynamics, such as flexible modes and nonlinearities) was guaranteed in ref. 15. However, time-domain performance of this design exhibits steady state tracking errors. The main contribution of the present article is the introduction of an additional controller term that eliminates the steady state error. Stability robustness and tracking performance of this new control scheme are also demonstrated with simulation examples.

In the next section, the mathematical model is described. Section 3 contains a brief discussion of robust stability and tracking performance problems, based on the control scheme proposed in ref. 15. In Section 4, simulation results are presented, and the new modified control structure is introduced to improve the steady state tracking performance. Concluding remarks are made in Section 5.

2. SYSTEM MODEL

In this article, we study two-dimensional motion of an n-link robot with a pair of musclelike actuators at every joint. For notational simplicity, we let $n = 3$ and consider a nonlinear *three*-link model of the biped in the sagittal plane (Fig. 1), with each of the links corresponding to a part of the musculoskeletal system. Link 1 (subscript 1) represents the two knees locked together; link 2 (subscript 2) represents the thighs locked together; and link three (subscript 3) represents the torso with arms, neck, and head together and considered stationary.

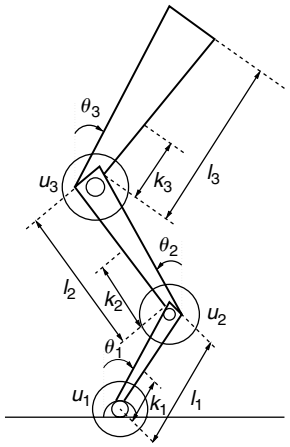

Figure 1. *Three*-link sagittal model of the leg, thigh, and trunk. The angles of the links are measured positive clockwise; the center of gravity of each link is measured relative to the lower hinge of the link; and the moments of inertia are relative to the center of gravity for each link.

2.1. Nonlinear Model

The dynamics of the system are derived using the Newton-Euler method (as detailed in ref. 14) and have a typical second-order nonlinear differential equation of the form

$$J(\Theta)\ddot{\Theta} + B(\Theta, \dot{\Theta})\dot{\Theta} + gG(\Theta) = EU_0 \qquad (1)$$

where $\Theta = [\theta_1 \ \theta_2 \ \theta_3]^T$ and $\dot{\Theta} = (d/dt)\Theta$ are the position and velocity, $J(\Theta)$ is the positive-definite symmetric moment of the inertia matrix, $B(\Theta, \dot{\Theta})$ is the vector of coriolis and centripetal forces, $G(\Theta)$ is the gravity vector, E is the torque input map matrix, U_0 is the applied joint torque vector, and g is the gravity constant (9.81 m/s^2). The nonlinear maps J, B, G, and E are given as follows:

$$J(\Theta) = \begin{bmatrix} I_1 + m_1k_1^2 + (m_2 + m_3)\ell_1^2 & (m_2k_2 + m_3\ell_2)\ell_1\cos(\theta_2 - \theta_1) & m_3k_3\ell_1\cos(\theta_3 - \theta_1) \\ (m_2k_2 + m_3\ell_2)\ell_1\cos(\theta_2 - \theta_1) & I_2 + m_2k_2^2 + m_3\ell_2^2 & m_3k_3\ell_2\cos(\theta_3 - \theta_2) \\ m_3k_3\ell_1\cos(\theta_3 - \theta_1) & m_3k_3\ell_2\cos(\theta_3 - \theta_2) & I_3 + m_3k_3^2 \end{bmatrix}$$

$$B(\Theta, \dot{\Theta}) = \begin{bmatrix} 0 & (m_2k_2 + m_3\ell_2)\ell_1\dot{\theta}_2\sin(\theta_1 - \theta_2) & m_3k_3\ell_1\dot{\theta}_3\sin(\theta_1 - \theta_3) \\ (m_2k_2 + m_3\ell_2)\ell_1\dot{\theta}_1\sin(\theta_2 - \theta_1) & 0 & m_3k_3\ell_2\dot{\theta}_3\sin(\theta_2 - \theta_3) \\ m_3k_3\ell_1\dot{\theta}_1\sin(\theta_3 - \theta_1) & m_3k_3\ell_2\dot{\theta}_2\sin(\theta_3 - \theta_2) & 0 \end{bmatrix}$$

$$G(\Theta) = \begin{bmatrix} -(m_1 + m_2\ell_1 + m_3\ell_1)\sin(\theta_1) \\ -(m_2k_2 + m_3\ell_2)\sin(\theta_2) \\ -m_3k_3\sin(\theta_3) \end{bmatrix} \qquad E = \begin{bmatrix} 1 & -1 & 0 \\ 0 & 1 & -1 \\ 0 & 0 & 1 \end{bmatrix}$$

2.2. Linear Model

In this article, we are interested in two-dimensional motion around the zero equilibrium point, $[\Theta^T \ \dot{\Theta}^T]^T = [0 \ 0]^T$. Let Θ_e be the equilibrium position vector of the *three*-link system, and Θ_p be the perturbation vector around the equilibrium point, that is, $\Theta = \Theta_e + \Theta_p \ \dot{\Theta} = \dot{\Theta}_p \ \ddot{\Theta} = \ddot{\Theta}_p$. Then (1) becomes

$$J(\Theta_e + \Theta_p)\ddot{\Theta}_p + B(\Theta_e + \Theta_p, \dot{\Theta}_p)\dot{\Theta}_p + gG(\Theta_e + \Theta_p) = EU_0 \tag{2}$$

Linearizing each of the nonlinear elements, neglecting higher-order terms and cross terms, and noting that $(\partial J/\partial\Theta)|_{\Theta_e} = 0$, $B(\Theta_e, \dot{\Theta}_e) = 0$, and $G(\Theta_e) = 0$, we obtain

$$J_o\ddot{\Theta} + g\left.\frac{\partial G}{\partial \Theta}\right|_{\Theta_e}\Theta = EU_0 \tag{3}$$

where

$$J(\Theta) \approx J(\Theta_e) = \begin{bmatrix} I_1 + m_1k_1^2 + (m_2 + m_3)l_1^2 & (m_2k_2 + m_3l_2)l_1 & m_3k_3l_1 \\ (m_2k_2 + m_3l_2)l_1 & I_2 + m_2k_2^2 + m_3l_2^2 & m_3k_3l_2 \\ m_3k_3l_1 & m_3k_3l_2 & I_3 + m_3k_3^2 \end{bmatrix}$$

$$B(\Theta_e + \Theta_p, \dot{\Theta}_p) \approx 0$$

$$G(\Theta) \approx \left.\frac{\partial G}{\partial \Theta}\right|_{\Theta_e}\Theta = \begin{bmatrix} -(m_1k_1 + m_3l_1 + m_3l_1) & 0 & \\ 0 & -(m_2k_2 + m_3l_2) & 0 \\ 0 & 0 & -m_3k_3 \end{bmatrix}\Theta$$

and $J_o := J(\Theta_e)$; here we have used $\Theta_p = \Theta$ for notational convenience.

It is known that this nonlinear time-delay system in natural systems is internally stable due to coactivation of the agonist-antagonist muscle pairs.[14] Intrinsic stability is achieved by position and velocity state feedback with appropriate gain matrices. The gain matrices are chosen to stabilize the system and influence the mechanical coupling between the links, so as to perform simultaneous and constrained/unconstrained motion for each of the links independently (i.e., decouple the system). For stability and feedback linearization, let $U_0 = E^{-1}(-K_i\Theta - L_i\dot{\Theta} + U)$, where U is the new external input variable, and K_i and L_i are respectively the position and velocity feedback gain matrices for intrinsic stability. The stable linearized system is then

$$J_o\ddot{\Theta} + L_i\dot{\Theta} + \left(g\left.\frac{\partial G}{\partial \Theta}\right|_{\Theta_e} + K_i\right)\Theta = U \tag{4}$$

and the transfer function for the linear system is

$$P(s) = (J_os^2 + L_is + K_o)^{-1} \tag{5}$$

where

$$K_o = K_i + g\left.\frac{\partial G}{\partial \Theta}\right|_{\Theta_e}$$

2.3. Time Delays

Suppose that the ith input ($i = 1, 2, 3$) to the plant is delayed by an ideal transmission delay of duration δ_i, corresponding to the neural transmission delays in the path of control (the efferent latency). Let $D_e(s)$ be a diagonal 3×3 matrix whose diagonal elements are $e^{-\delta_i s}$, where s is the Laplace transform variable. If $U_c(s)$ is the torque output of the controller, it follows that the input to the plant $U(s)$ is

$$U(s) = D_e(s)U_c(s)$$

Similarly, there is a transmission delay in the feedback path of the signals corresponding to the transmission delays from the muscle to the brain (the afferent latency). Let $D_a(s)$ be a diagonal $n \times n$ matrix with diagonal elements $e^{-\gamma_i s}$. If $z(s)$ is the output of the plant, the measured output signal available for feedback, z_a, is

$$z_a(s) = D_a(s)z(s)$$

3. STABILITY ROBUSTNESS AND TRACKING PERFORMANCE

Consider the standard feedback control framework depicted in Figure 2. It has been postulated that a controller structure, similar in function to the one here,

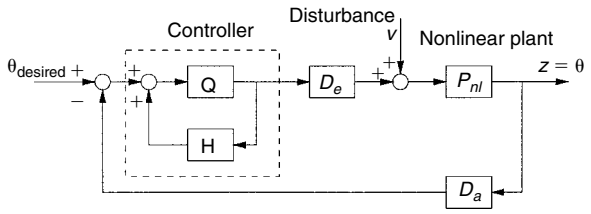

Figure 2. Block diagram of a closed-loop system. The controlled system consists of the dynamics of the three-link system with efferent (D_e) and afferent (D_a) path delays. The controller has a feed-forward element Q and a feedback element H.

exists in natural systems, for stability and synchronized motion of bodies in the presence of time delays.[32]

By virtue of the parameterization of all stabilizing controllers (see refs. 2, 11, 49, 30, and their references), the controller has a feedback configuration with a feedforward and a feedback term, as shown in Figure 2, Q and H being 3×3 transfer function matrices (see also refs. 36 and 46). In ref. 15, the free parameter Q and the plant model H are determined by solving an inverse problem as follows. Let the desired closed-loop input-output map from the reference input Θ_{desired} to the position output Θ be the linear map defined by

$$T_{cl_{\text{desired}}} = T_d D_d = D_d T_d \tag{6}$$

where $T_d(s)$ is a diagonal rational transfer matrix (for decoupling) and $D_d(s)$ is a diagonal matrix whose entries are $e^{-\lambda_i s}$. The actual nonlinear input-output map of the closed-loop system in Figure 2 is

$$T_{cl} = P_{nl} D_e (I - QH + QD_a P_{nl} D_e)^{-1} Q$$

where P_{nl} is the locally stable (around $\Theta = 0$, $\dot{\Theta} = 0$) nonlinear input-output map from U to Θ defined by

$$J(\Theta)\ddot{\Theta} + (B(\Theta, \dot{\Theta}) + L_i)\dot{\Theta} + (K_i\Theta + gG(\Theta)) = U \tag{7}$$

Following the guidelines of controller parameterizations,[2,30] let H be the plant seen by the controller, that is,

$$H = D_a P_{nl} D_e$$

which leads to the input-output map

$$T_{cl} = P_{nl} D_e Q$$

Since $T_{cl_{\text{desired}}}$ is diagonal, Q can be chosen such that overall time delays in each channel are equal (for a synchronized motion). Hence, $D_d(s)$ should be taken as $D_d(s) = e^{-\lambda s} I$, where I denotes the 3×3 identity matrix. With this choice for $D_d(s)$, to get $T_{cl_{\text{desired}}} = T_{cl}$, we must have

$$Q = D_q P_{nl}^{-1} T_d \quad \text{where}$$
$$D_q(s) = \text{diag}\left(e^{-(\lambda-\delta_1)s} \cdots e^{-(\lambda-\delta_3)s}\right)$$

with $\lambda = \max\{\delta_1, \delta_2, \delta_3\}$. Note that P_{nl} is a nonlinear map and its inverse, in general, does not exist; so, in the implementation of Q, we use the linear approximation $P_{nl} \approx P$. Since Q must be a stable proper operator, T_d must be such that $P^{-1}(s)T_d(s)$ is stable and proper. Thus the controller design is reduced to finding the "desired" closed-loop transfer matrix $T_d(s)$ satisfying certain performance and robustness objectives, subject to the condition that $P^{-1}(s)T_d(s)$ is stable and proper.

Following the guidelines of ref. 15 for guaranteed stability robustness and nominal (for the linearized plant) tracking performance, the $\mathcal{H}^\infty$ problem defined as follows is solved to determine the optimal T_d:

$$\gamma_{\text{opt}} = \inf_{T_d \in \mathcal{H}^\infty} \left\| \begin{bmatrix} (I - T_d D_d D_a) W_1 \\ T_d D_d D_a W_2 \end{bmatrix} \right\|_\infty \tag{8}$$

where $W_1(s)$ and $W_2(s)$ are defined as

$$\left.\begin{aligned} \|W_1(j\omega)\|^2 &\geq \|W_{\text{ref}}(j\omega)\|^2 + \|W_{\text{unmodel}}(j\omega)\|^2 \\ \|W_2(j\omega)\|^2 &\geq \|P^{-1}(j\omega)W_{\text{unmodel}}(j\omega)\|^2 \\ &\quad + \|W_{\text{delay}}(j\omega)\|^2 \end{aligned}\right\} \quad \forall\omega \tag{9}$$

with W_{ref} being a weighting matrix determined by the class of reference inputs of interest, W_{delay} the weighting matrix determined from the delay uncertainty, and W_{unmodel} the uncertainty weight (determined from the unmodeled high-frequency dynamics, and from neglected nonlinear dynamics; see refs. 15 and 21 for details).

Note that the problem defined in (8) can be seen as a mixed-sensitivity minimization problem for the fictitious "plant" $P_f = W_2^{-1} D_a D_d$ and the associated feedback "controller" $C_f = T_d W_2 (I - T_d D_d D_a)^{-1}$; and that, as formulated, the problem can be solved using the results appearing in refs. 11 and 44. Thus the

desired transfer matrix, $T_d(s)$, is calculated from the optimal solution, C_f, of this mixed-sensitivity problem; that is,

$$T_d(s) = (I + P_f(s)C_f(s))^{-1}C_f(s)W_2(s)^{-1} \qquad (10)$$

4. SIMULATION EXAMPLES AND 2-DOF CONTROL SCHEME

A point-to-point, and a periodic movement are considered to illustrate the performance of the control design scheme outlined in the preceding. The point-to-point motion is a squatting maneuver, for which the reference inputs are the desired angular positions of the leg, thigh, and trunk. The reference position trajectory generator is varied smoothly between the initial and final values using a sinusoidal function (see Fig. 3). This guarantees smooth velocity and acceleration profiles and there is no excessive demand for accelerating torques on the actuators. For a periodic movement the system is subjected to periodic trajectories of fixed amplitude and frequency (these are determined from the desired end position of the links for a rocking motion, and the dynamics of the system).

Table I. System parameters.

	Link 1	Link 2	Link 3
Mass (kg)	5.05	18.67	41.87
Moment of inertia (kg/m^2)	0.17	0.50	2.10
Length of the link (m)	0.401	0.412	0.619
Center of gravity (m)	0.21	0.26	0.24

The physical parameters of the three-link biped corresponding to an average-sized human being are defined in Table I.[14] The position and velocity feedback gain matrices for intrinsic stability of the system are taken from ref. 14:

$$L_i = \begin{bmatrix} 39.147070 & 0 & \\ 0 & 16.2630 & 0 \\ 0 & 0 & 6.3434 \end{bmatrix},$$

$$K_i = \begin{bmatrix} 509.5364 & 0 & 0 \\ 0 & 325.2665 & 0 \\ 0 & 0 & 140.8677 \end{bmatrix}$$

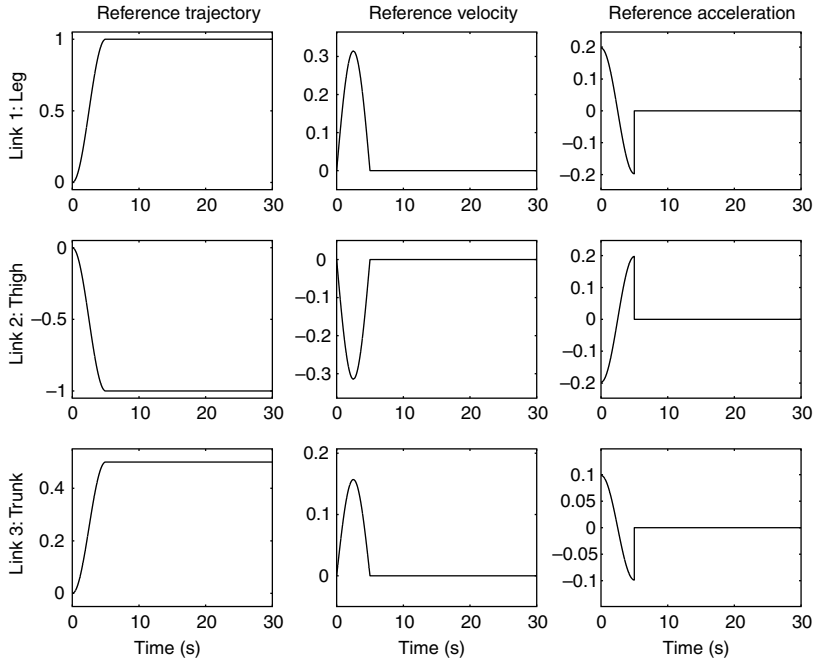

Figure 3. Reference input trajectory (angles), desired velocity, and acceleration for a squatting maneuver.

For these numerical values, the system matrices $\{A,\ B,\ C\}$ defining $P(s) = C(sI - A)^{-1}B$ are

$$A = \begin{bmatrix} 0 & 0 & 0 & 1 & 0 & 0 \\ 0 & 0 & 0 & 0 & 1 & 0 \\ 0 & 0 & 0 & 0 & 0 & 1 \\ -206.4031 & 87.3725 & -1.4012 & -30.9605 & 13.1059 & -0.2102 \\ 210.3160 & -110.4128 & 9.0816 & 31.5474 & -16.5619 & 1.3622 \\ -8.6476 & 23.2832 & -16.4552 & -1.2971 & 3.4925 & -2.4683 \end{bmatrix}$$

$$B = \begin{bmatrix} 0 & 0 & 0 \\ 0 & 0 & 0 \\ 0 & 0 & 0 \\ 0.7909 & -0.8059 & 0.0331 \\ -0.8059 & 1.0184 & -0.2148 \\ 0.0331 & -0.2148 & 0.3891 \end{bmatrix}, \qquad C = \begin{bmatrix} 1 & 0 & 0 & 0 & 0 & 0 \\ 0 & 1 & 0 & 0 & 0 & 0 \\ 0 & 0 & 1 & 0 & 0 & 0 \end{bmatrix}$$

$$\text{Poles of } P(s) = -37.2794 \quad -8.1185 \quad -1.8894 \pm 4.6500i \quad -0.4069 \pm 2.2935i$$

- For periodic references:

$$W_1(s) = \frac{1.215s^6 + 5.887s^5 + 17.65s^4 + 23.72s^3 + 27.78s^2 + 80.65s + 84}{s^6 + 10.5s^5 + 36.9s^4 + 46.15s^3 + 14.42s^2 + 16.58s + 0.0017} I$$

$$W_2(s) = \frac{0.093s^8 + 0.53s^7 + 1.8s^6 + 3.07s^5 + 2.44s^4 + 3.2s^3 + 2.85s^2 + 0.58s + 0.0042}{s^3 + 1.97s^2 + 1.21s + 0.24} I$$

The values for the time delays in each channel (link) are taken to be

$$\delta_1 = \gamma_1 = 0.08 \text{ s}, \quad \delta_2 = \gamma_2 = 0.06 \text{ s}, \quad \delta_3 = \gamma_3 = 0.04 \text{ s}$$

Therefore λ is chosen as $\lambda = 0.08$ s. The desired closed-loop transfer matrix (10) is derived from the solution to the previously mentioned mixed-sensitivity minimization problem with the following numerical values of the uncertainty weights.

These numerical values are determined from the guidelines set in ref. 15 for weight selection; they are chosen for a good trade-off between stability robustness and tracking performance. The resulting high-order $T_d(s)$ is approximated by a low-order transfer function using balanced and truncated realization, discussed in refs. 12 and 33. For these numerical

- For step-like references:

$$W_1(s) = \frac{3.479s^4 + 11.06s^3 + 39.3s^2 + 92.62s + 84}{s^4 + 10.5s^3 + 36.5s^2 + 42s + 0.0042} I$$

$$W_2(s) = \frac{0.265s^6 + 0.9477s^5 + 2.128s^4 + 4.736s^3 + 3.94s^2 + 0.792s + 0.0042}{s^3 + 1.972s^2 + 1.21s + 0.24} I$$

values, the resulting relatively low-order $T_d(s)$ are as follows.

- For step-like references:

$$T_d(s) = \text{diag}\left[\begin{array}{c} \dfrac{24.63s^4 - 613s^3 + 5.954e04s^2 + 6.353e04s + 1.562e04}{s^7 + 31.68s^6 + 2612s^5 + 1.455e04s^4 + 4.732e04s^3 + 1.19e05s^2 + 7.925e04s + 1.562e04} \\ \dfrac{24.72s^4 - 609.9s^3 + 5.946e04s^2 + 6.887e04s + 2.002e04}{s^7 + 31.62s^6 + 2603s^5 + 1.466e04s^4 + 4.802e04s^3 + 1.22e05s^2 + 8.883e04s + 2.002e04} \\ \dfrac{24.18s^4 - 598.6s^3 + 6.015e04s^2 + 6.576e04s + 1.712e04}{s^7 + 31.56s^6 + 2682s^5 + 1.493e04s^4 + 4.883e04s^3 + 1.225e05s^2 + 8.335e04s + 1.712e04} \end{array}\right]$$

- For periodic references:

$$T_d(s) = \text{diag}\left[\begin{array}{c} \dfrac{-0.034s^6 + 0.7s^5 - 7.423s^4 + 52.13s^3 + 1607s^2 + 606s + 432.5}{s^8 + 26.38s^7 + 159.1s^6 + 605.7s^5 + 1363s^4 + 2021s^3 + 2060s^2 + 1312s + 433.6} \\ \dfrac{-0.035s^6 + 0.72s^5 - 7.58s^4 + 53.1s^3 + 1545s^2 + 588.7s + 417.2}{s^8 + 26.11s^7 + 156.6s^6 + 594.5s^5 + 1333s^4 + 1970s^3 + 2001s^2 + 1269s + 416.2} \\ \dfrac{-0.035s^6 + 0.704s^5 - 7.43s^4 + 51.87s^3 + 1516s^2 + 583.6s + 411.3}{s^8 + 26.06s^7 + 156s^6 + 591.9s^5 + 1324s^4 + 1956s^3 + 1982s^2 + 1255s + 410.1} \end{array}\right]$$

4.1. Point-to-Point Motion

Two simulations of the three-link model just described were performed for point-to-point movement. Simulation results were documented graphically, displaying the output positions, angular velocity, acceleration, input torques, and the phase plane of the three links of the biped. In the first simulation (see Fig. 4), the feedback component H of the controller is designed as a linear element, $H = D_a P D_e$, where P is the linear model of the plant; whereas in the second simulation (see Fig. 5), the nonlinear model of the plant is implemented in $H = D_a P_{nl} D_e$. For both cases the feedforward component Q is linear, $Q(s) = D_q(s) P^{-1}(s) T_d(s)$, so that in the vicinity of the vertical stance, the three links are decoupled and the system is stable; $P^{-1}(s)$ is the linear plant model inverse; and $T_d(s)$ and $D_q(s)$ are as previously defined.

As may be seen from the phase portrait of the system with the linear feedback element H (see Fig. 4), stability may be lost as the robustness condition stated in ref. 15 is not met. Although the response is oscillatory in acceleration and velocity, position tracking is fairly good and the average steady state error is negligible. The oscillations are more prominent in link 3 (the trunk), which has the maximum weight and the highest moment of inertia. The simulation results for the case in which H uses the nonlinear plant model (see Fig. 5) suggest that the system is stable and the robustness objectives are met, but there is a significant steady state error as the position does not reach its desired steady state value.

4.2. Additional Controller Term

The aforementioned tracking error is due to the fact that the linear plant model inverse, P^{-1}, is used in the implementation of Q, rather than the exact nonlinear inverse P_{nl}^{-1}; so the input compensates for the linearized gravity term $g\Theta$ rather than $g\sin(\Theta)$. To eliminate this problem, we propose to add a new feedback term to the controller. First, recall that the locally stable nonlinear plant equation is

$$J(\Theta)\ddot{\Theta} + B(\Theta, \dot{\Theta})\dot{\Theta} + gG(\Theta) = U - L_i\dot{\Theta} - K_i\Theta$$

while $P^{-1}(s) := J_o s^2 + L_i s + K_o$. Assuming that the feedback system is stable and in steady state, (i.e., $\dot{\Theta} = 0$ and $\ddot{\Theta} = 0$), the torque requirement of the biped is $U_{ss} = gG(\Theta) + K_i\Theta$, where K_i is the position feedback gain matrix. Since $G(\Theta) = K_G \sin\Theta$, we have

$$U_{ss} = gK_G \sin\Theta + K_i\Theta \tag{11}$$

where $K_G = \text{diag}[-(m_1k_1 + m_3l_1 + m_3l_1), -(m_2k_2 + m_3l_2), -m_3k_3]$. On the other hand, the output of the linear plant inverse model $P^{-1}(s)$ under steady state conditions is $U_s = K_o\Theta$, where $K_o = (K_i + gK_G)$. Thus, the steady state torque input is

$$U_s = (K_i + gK_G)\Theta \tag{12}$$

As the required torque U_{ss} is not being supplied to the plant by U_s, the output does not track the reference input. Note that the steady state error,

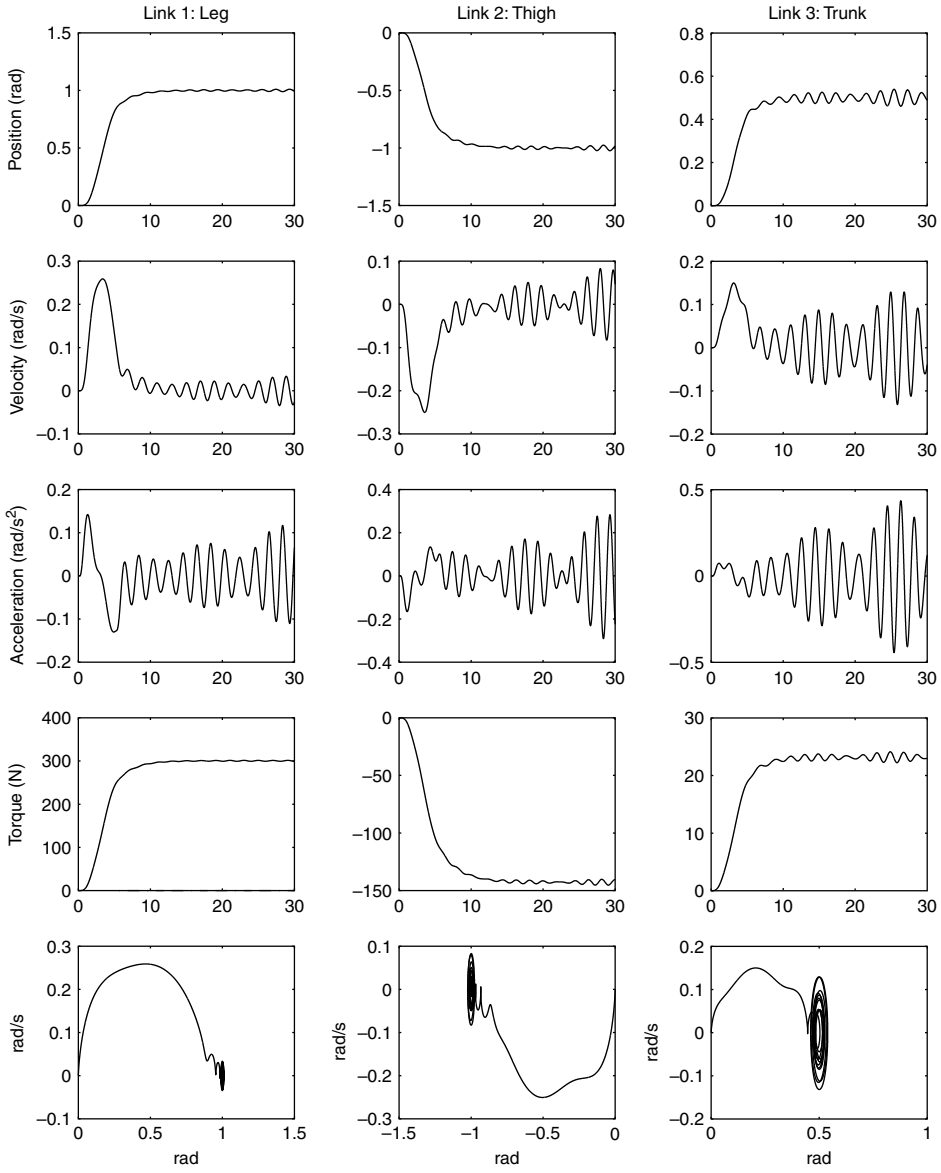

Figure 4. Output angular position, velocity, acceleration, and musclelike actuator torque input to the plant for the squatting maneuver with the linear model of the plant H. The phase portraits show the limit cycle for this design.

$\Delta_\Theta := \lim_{t\to\infty}(\Theta_{\text{desired}}(t) - \Theta(t))$, can be quantified as

$$\Delta_\Theta = (I - K_i^{-1}K_G)(\sin(\Theta_f) - \Theta_f) \tag{13}$$

where $\Theta_f = \lim_{t\to\infty}\Theta_{\text{desired}}(t)$. The values for the steady state error in Figure 5 are

$$\Delta_\Theta = [-0.1739, \quad 0.1908, \quad -0.0255]^T$$

which represent approximate undershoots of 17% in link 1, 19% in link 2, and 5% in link 3; these numerical results match the formula for Δ_Θ in (13).

Based on the preceding discussion, to eliminate the steady state error we must add a correction torque

$$U_{\text{corr}} = gK_G(\sin\Theta - \Theta) \tag{14}$$

to the controller output. Here we propose to implement this correction torque as a nonlinear function acting on the filtered version of the output Θ. This block is implemented as shown in Figure 6, where the output Θ is assumed to be delayed by D_s. In most telerobotics

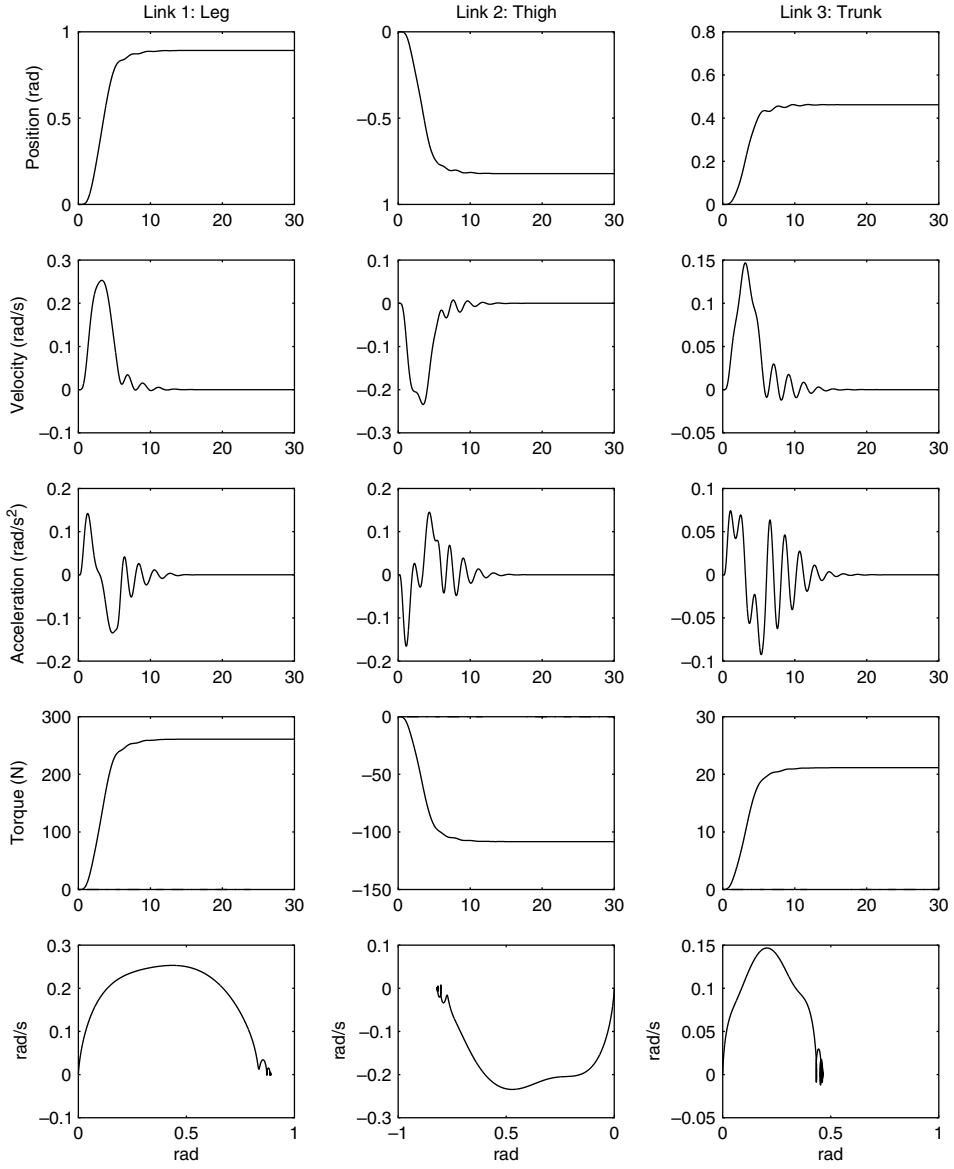

Figure 5. Output angular position, velocity, acceleration, and musclelike actuator torque input to the plant for the squatting maneuver with the nonlinear model of the plant in H. Phase portraits illustrate the stability of the system.

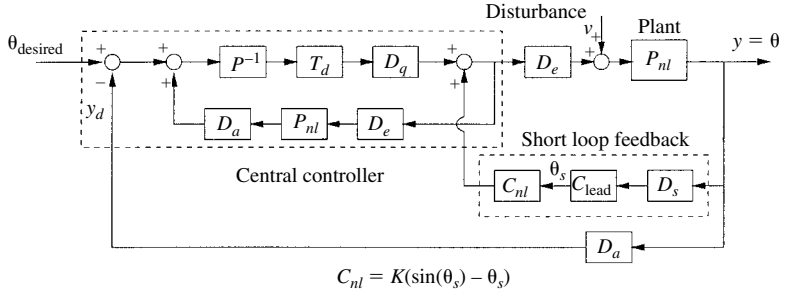

Figure 6. Nonlinear controller, nonlinear plant model with short loop feedback for gravity correction.

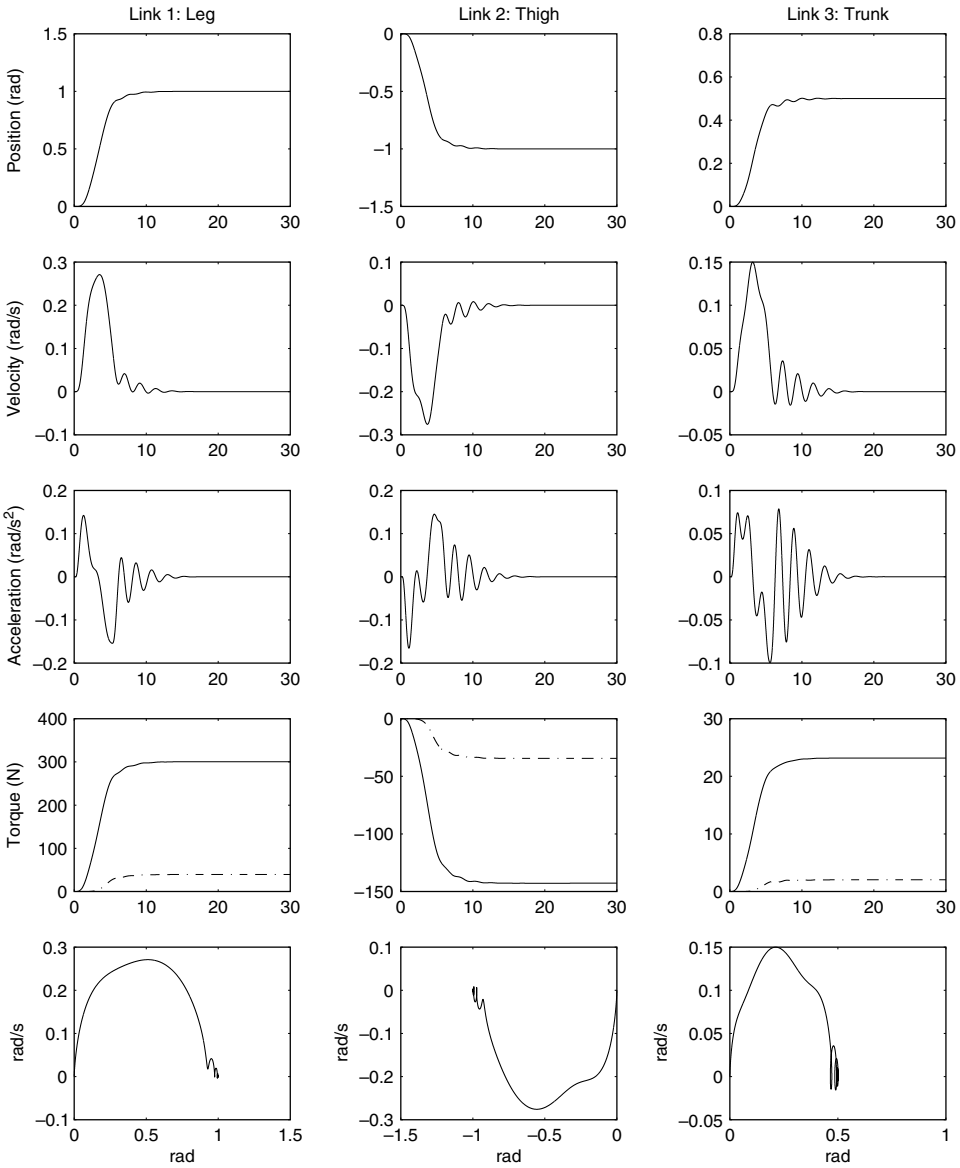

Figure 7. Output angular position, velocity, acceleration, and musclelike actuator torque input to the plant for squatting maneuver with nonlinear correction model. Phase portraits explain the stability of the system.

applications $D_s = D_a$ that is, the correction is implemented by the central controller, which is far away from the robot. However, in neural control of musculoskeletal (biological) systems, the correction term can be viewed as a short loop feedback compensator, separate from the CNS (e.g., spindle feedback[16]); in that case the delays in D_s can be as small as half the amount of the delays in D_a. In either case, a first-order lead compensator, $C_{\text{lead}} = (1 + \alpha\tau s)/(1 + \tau s)$ with $\tau > 0$ and $\alpha > 1$, is put in cascade to compensate the phase lag due to D_s and to recover/predict the nondelayed value of Θ. Then, the correction torque can be generated by the nonlinear compensator $C_{nl} = K(\sin(\Theta_s) - \Theta_s)$, with $K = gK_G$, by making the approximation $\Theta_s \approx \Theta$.

Simulations for a squatting maneuver are performed with the system model of Figure 6, by taking $D_s = 0.5D_a$. As seen in Figure 7 (where U_{corr} is shown by the dotted lines), for small values of the angular position Θ we have $\sin\Theta \approx \Theta$, hence the correction torque U_{corr} is negligible in the initial stages of the motion. However, as the angular position increases, the difference becomes significant, and this necessitates larger correction torque.

4.3. Rhythmic Motion

Since movements such as walking, running, and dancing are inherently rhythmic, the study of rhythmic motion is crucial to understanding how the body controls such movements, and will also help in implementing rhythmic movements for robots and walking machines. The frequency (rhythm) of the motion is governed by the bandwidth of the system. For the nonlinear system defined by the numerical values given previously, the bandwidth was analyzed empirically by subjecting the system to a series of small amplitude signals of different frequencies and observing the response of the system to these inputs. The range of frequencies the system can track perfectly will give an idea of the bandwidth of the system. The reference signal to the system was $\theta = 0.1[\sin\omega t \ -\sin\omega t \ \sin\omega t]$ and we varied the input signal frequency ω from 0. From the response of the system to various input frequencies it was concluded that the output tracks the input satisfactorily for input frequencies ranging from 0 to 0.2π. Hence it can concluded that the empirical bandwidth of the system is 0.2π rad/s.

We analyzed the system response to a periodic input by simulating the rocking maneuver performed by a human. The reference signal for this motion is $\Theta_{\text{desired}}(t) = [-0.1\sin 0.2\pi t \ \ 0.2\sin 0.2\pi t \ \ 0.5\sin 0.2\pi t]$, where the amplitude is the final value of the angular position for the joints. The reference trajectory and the output angles of the system in Figure 6 are shown in Figure 8. The system tracks the reference with a phase lag introduced due to the delay in the system.

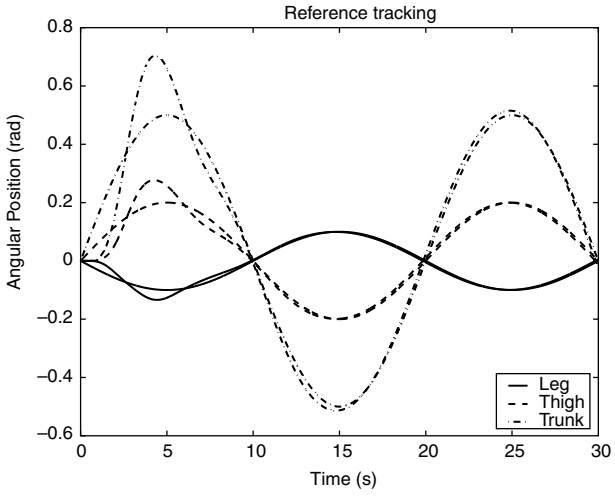

Figure 8. Rocking maneuver performed with nonlinear controller and short loop feedback for gravity correction.

5. CONCLUSION

The ultimate goal of our work is to understand the control mechanism present in the human CNS and to develop a physiologically equivalent controller. The ideas of this article can also be used in telerobotics, where time delay compensation is a key issue. We have extended the results of ref. 15 and proposed a new control scheme. The approach presented here partitions the controller into a forward path controller, which is a model-matching type with a feedforward and feedback element, and a short loop feedback controller. As in ref. 15, the feedforward element Q is determined from an $\mathcal{H}^\infty$ optimal control problem (to meet stability robustness and tracking performance requirements), whereas the feedback element H is the exact model of the controlled plant and provides a predictive mechanism for control. The novelty in this article is the introduction of the short loop feedback controller, which provides gravity compensation due to the linear plant model inverse in Q. This approach does not require that we realize the nonlinear plant inverse in the forward path controller, and makes the control scheme feasible and practically realizable.

It is noteworthy that, based on these theoretical developments, the short loop feedback appears to control the stiffness of the system (as described by Eq. (14)). It has been experimentally known for some time[32] that the spindle feedback and spinal reflexes in natural systems are utilized for stiffness control. Therefore, the theoretical findings of this article confirm past experimental results regarding the function of spinal reflexes.

Simulations for a three-link sagittal system driven by moment-of-force generators for a squatting and rocking maneuver were performed to test the control scheme. It should be noted that the system model was kept simple to illustrate the principle behind the algorithm and not introduce complex mathematical equations. The method developed here can be extended to complex system models with links representing every body part, and including additional disturbances introduced by neglected dynamics and body movement. A more detailed model of the muscle actuators will affect the exact values of the muscle forces and the system dynamics, but the basic idea of the control strategy developed here remains the same, provided that these models can be implemented in different parts of the controller.

As stated in the Introduction, it is not our intention to hypothesize that the CNS utilizes mechanisms advanced in this paper. Our objective is to provide a functioning linear controller for implementing

simple motions. As a byproduct, this may afford computational[22] and analytical understanding of some workings of the CNS, in contrast to studies that offer insight into neural structures and requirements comparison.[24,25]

Finally, addition of a feedforward component to our model could potentially improve the performance of the system, and allow the use of several linearization schemes along the trajectory, and gain programming.[23] However, optimization of system performance was not an objective, even though natural systems seem to have a feedforward component due to coactivation.[14,24,25]

ACKNOWLEDGMENT

This work was, in part, supported by the Fundamental Research Laboratories (FRL) of Honda R&D Americas, Inc., Mountain View, California.

REFERENCES

1. C.H. An and J.M. Hollerbach, The role of dynamic models in Cartesian force control and manipulation, Int J Robot Res 8 (1989), 51–72.
2. V. Anantharam and C.A. Desoer. On the stabilization of nonlinear systems, IEEE Trans Automat Contr 29 (1984), 569–572.
3. M.A. Arbib, P. Erdi, and J. Szentagothai, Neural organization, structure, function and dynamics, MIT Press, Cambridge, MA., 1998.
4. A. Bahill and J. McDonald. Model emulates human smooth pursuit system producing zero latency tracking, Biological Cybernetics 48 (1983), 213–222.
5. A. Banerjee, et al. A behavioral layer architecture for telecollaborative virtual manufacturing operations, IEEE Trans Robot Automat 16 (2000), 218–227.
6. J.S. Bay, Fundamentals of Linear State Space Systems. WCB/McGraw-Hill, Boston, 1999.
7. L. Conway, R.A. Volz, and M.W. Walker, Teleautonomous systems: Projecting and coordinating intelligent action at a distance, IEEE Trans Robot Automat 6 (1990), 146–158.
8. J. Doeringer and N. Hogan, Serial processing in human movement production, Neural Networks 11 (1998), 1345–1356.
9. A. Eusebi and C. Melchiorri, Force reflecting telemanipulators with time-delay: Stability analysis and control design, IEEE Trans Robot Automat 14 (1998), 635–640.
10. W.R. Ferrell, Delayed force feedback, Human Factors (1966), 449–455.
11. C. Foias, H. Özbay, and A. Tannenbaum. Robust control of infinite dimensional systems: Frequency domain methods, LNCIS 209, Springer-Verlag, London, 1996.
12. G. Gu, P.P. Khargonekar, and E.B. Lee, IEEE Trans Automat Contr 34 (1989), 610–618.
13. J.K. Hale and S.M.V. Lunel, Introduction to functional differential equations. New York: Springer-Verlag, 1993.
14. H. Hemami and J.A. Dinneen, A Marionette-based control strategy for stable movement, IEEE Trans System Man Cybernet 23 (1993), 502–511.
15. H. Hemami and H. Özbay. Modeling and control of biological systems with multiple afferent and efferent transmission delays, J Rob Syst 17:(11) (2000), 609–622.
16. J.C. Houk, P.E. Crago, and W.Z. Rymer, Function of the spindle dynamic response in stiffness regulation—a predictive mechanism provided by nonlinear feedback, Muscle Receptors and Movement, H. Taylor and A. Prochazka (Editor), MacMillan, London, 1981, pp. 299–309.
17. R.J. Jagacinski, M.W. Burke, and D.P. Miller, Use of schemata and acceleration information in stopping a pendulum-like system, J Experimental Psychology: Human Perception and Performance 3 (1977), 212–223.
18. R.J. Jagacinski and D.P. Miller, Describing the human operator's internal model of a dynamic system, Human Factors 20 (1978), 425–433.
19. R.J. Jagacinski and S. Hah, Progression-regression effects in tracking repeated patterns, J Experimental Psychology: Human Perception and Performance 14 (1988), 77–88.
20. T. Kailath, Linear Systems, Prentice Hall, Englewood Cliffs, NJ, 1980.
21. A. Kataria, H^{∞} Controller Design for Neuromusculoskeletal Systems with Multiple Afferent and Efferent Transmission Delays, M.S. dissertation, Department of Electrical Engineering, The Ohio State University, 1999.
22. M. Katayama, A computational understanding of motor learning control using neural internal models for a multi-joint arm, Ph.D. dissertation, Faculty of Engineering, University of Tokyo, November 1993.
23. A. Katbab and H. Hemami, The role of gain programming in the voluntary movement of the human forearm, Medical and Biological Engineering and Computing, 23 (1985), 230–236.
24. M. Kawato, K. Furukawa, and R. Suzuki, A hierarchical neural network model for control and learning of voluntary movement, Biological Cybernetics, 57 (1987), 169–185.
25. J. Kim and H. Hemami, Coordinated three-dimensional motion of the head and torso by dynamic neural networks, IEEE Tran Syst Man Cybernet Part B, Cybernetics 28:(5) (1998), 653–666.
26. D.A. Lawrence, Stability and transparency in bilateral teleoperations, IEEE Trans Robot Automat 9 (1993), 624–637.
27. S. Lee, H.S. Lee, Intelligent control of manipulators interacting with an uncertain environment based on generalized impedance, Proc 6th IEEE Int Symp Intelligent Control, August 1991, pp. 61–66.
28. S. Lee, H.S. Lee, Modeling, design and evaluation of advanced teleoperator control system with short time delay, IEEE Trans Robot Automat 9 (1993), 607–623.
29. A. Liu, G. Tharp, L. French, S. Lai, and L. Stark, Some of what one needs to know about using head-mounted displays to improve teleoperator performance, IEEE Trans Robot Automat 9 (1993), 638–648.
30. W.M. Lu, A state-space approach to parameterization of stabilizing controllers for nonlinear systems, IEEE Trans Automat Contr 40 (1995), 1579–1588.

31. R.J. Mayhan, Discrete-time and continuous-time linear systems, Addison Wesley, Reading, MA, 1984.
32. R.C. Miall, D.J. Weir, D.M. Wolpert, and J.F. Stein, Is the cerebellum a Smith Predictor? J Motor Behavior 25 (1993), 203–216.
33. B.C. Moore, Principal component analysis in linear systems: Controllability, observability and model reduction, IEEE Trans Automat Contr 26 (1981), 17–31.
34. F.A. Mussa-Ivaldi and E. Bizzi, Learning Newtonian Mechanics, self-organizational computational maps, P. Morasso and V. Sanguineti (Editors), Advances in Psychology, Vol. 119, Elsevier, Amsterdam, 1997, pp. 191–237.
35. H. Özbay, Introduction to Feedback Control Theory. CRC Press, Boca Raton, FL, 2000.
36. H. Özbay, $\mathcal{H}^\infty$ optimal controller design for a class of distributed parameter systems, Int J Contr 58 (1993), 739–782.
37. H. Özbay, S. Kalyanaraman, and A. İftar, On rate-based congestion control in high-speed networks: Design of an H^∞ based flow controller for single bottleneck, Proc American Control Conf, Philadelphia, PA, June 1998, pp. 2376–2380.
38. M.G. Paulin, A method for analysing neural computation using receptive fields in state space, Neural Networks 11 (1998), 1219–1228.
39. A. Pellionisz and R. Llinas, Brain modeling by tensor network theory and computer simulation, the cerebellum: Distributed processor for predictive coordination, Neuroscience 4 (1979), 323–348.
40. C.P. Sayers, Intelligent image fragmentation for teleoperations over delayed low-bandwidth links, Proc IEEE Int Conf on Robotics and Automation, Minneapolis, April 1996, pp. 1363–1368.
41. T.B. Sheridan, Space teleoperations through time delay: Review and prognosis, IEEE Trans Robot Automat 9 (1993), 592–606.
42. O.J.M. Smith, Feedback control systems. McGraw-Hill, New York, 1958.
43. G. Stepan, Retarded Dynamical Systems: Stability and characteristic functions, Longman Scientific & Technical, New York: Wiley, 1989.
44. O. Toker and H. Özbay, $\mathcal{H}^\infty$ Optimal and suboptimal controllers for infinite dimensional SISO plants, IEEE Trans Automat Contr 40 (1995), 751–755.
45. J. van Heijst, J.E. Vos, and D. Bullock, Development of biologically inspired spinal neural network for movement control, Neural Networks 11 (1998), 1305–1316.
46. M. Vidyasagar, Control system synthesis: A factorization approach, MIT Press, Cambridge MA, 1985.
47. M.M. Wloka, Lag in multi-processor virtual reality, Presence 4 (1995), 50–63.
48. N. Xi and T.J. Tarn, Action synchronization and control of internet based telerobotic systems, Proc IEEE Int Conf on Robotics and Automation Detroit, MI, May 1999, pp. 219–224.
49. K. Zhou, J.C. Doyle, and K. Glover, Robust Optimal Control, Prentice Hall, New York, 1996.